

# Inhibition of HIV-1 Ribonuclease H Activity by Novel Frangula-Emodine Derivatives

Kharlamova Tatyana<sup>1</sup>, Esposito Francesca<sup>2</sup>, Zinzula Luca<sup>2</sup>, Floris Giovanni<sup>2</sup>, Cheng Yung-Chi<sup>3</sup>, E. Dutschman Ginger<sup>3</sup> and Tramontano Enzo<sup>2,\*</sup>

<sup>1</sup>A.B. Bekturov Institute of Chemical Sciences, 050010, Almaty, Kazakhstan; <sup>2</sup>Department of Applied Sciences in Biosystems, University of Cagliari, I-09042, Monserrato, Italy; <sup>3</sup>Department of Pharmacology, Yale University School of Medicine, 06510, New Haven, CT, USA

**Abstract:** The HIV-1 reverse transcriptase (RT) associated ribonuclease H (RNase H) activity hydrolyzes the RNA component of the viral heteroduplex RNA:DNA replication intermediate. Even though this function is essential for viral replication, until now only very few compounds have been reported to inhibit it. Anthraquinones are common secondary metabolites which have diverse biological activities. In particular, some of them have been reported to inhibit the HIV-1 RT polymerase and integrase activities in biochemical assays. Given the structural similarities between integrase and RNase H proteins, we synthesized a series of frangula-emodine derivatives and showed that the introduction of a bromine atom in position 7 of the anthraquinone structure leads to derivatives which are able to inhibit both HIV-1 polymerase and RNase H functions at micromolar concentrations. Mechanism of action studies performed on the 7-brom-6-O-phenacyl-1,8-dihydroxy-3-methyl anthraquinone (K67) showed that this compound is a non-competitive inhibitor of the RNase H function and that it binds to a site which is not overlapping to the non-nucleoside RT inhibitors binding site. This study demonstrates that anthraquinone derivatives may be a scaffold to be further developed to obtain selective HIV-1 RNase H inhibitors and represent a new step toward the identification of new anti-RT agents.

**Key Words:** HIV-1, Ribonuclease H, RNase H, Drug discovery, Anthraquinones, Enzyme inhibition, Reverse transcriptase, RT.

## INTRODUCTION

The human Immunodeficiency type 1 (HIV-1) reverse transcriptase (RT) is a viral-coded enzyme which catalyzes the conversion of the viral single-stranded genomic RNA into a double-stranded DNA. In order to accomplish this composite process, RT executes two distinct associated activities: *i*) a DNA polymerase activity which recognizes both RNA and DNA as templates and *ii*) a degradative activity, termed ribonuclease H (RNase H), that hydrolyzes the RNA component of the heteroduplex RNA:DNA replication intermediate. The two RT-associated enzymatic functions are carried out by two distinct catalytic sites which are separated by a distance of approximately 18 base pairs from each other and are functionally strictly related [1-3].

Both RT-associated activities are required for DNA provirus formation and HIV replication [2,3]. In fact, mutations that selectively impair the RNase H function abolish the HIV infectivity [4]. Hence, the RT-associated RNase H function is an attractive target for the development of new antiretroviral agents [3,5]. In spite of this, however, the vast majority of compounds targeting the HIV-1 RT are actually inhibitors of its associated DNA polymerase activity and only a very few inhibit its RNase H activity [5]. Among these few, there are the diketo acid (DKA) derivatives 4-[5-(benzoylamino)thien-

2-yl]-2,4-dioxobutanoic acid (BTDBA, Fig. 1) [6] and the 6-[1-(4-fluorophenyl)methyl-1H-pyrrol-2-yl]-2,4-dioxo-5-hexenoic acid ethyl ester (RDS 1643, Fig. 1) [7] which were synthesized within two independent anti-HIV drug-development programs originally focused on anti-integrase inhibitors. In fact, given that integrase and RNase H belong to the polynucleotidyl transferase family and share structural similarities, these DKA derivatives were also tested on the HIV-1 RT-associated functions and found to inhibit this activity in the low micromolar range (IC<sub>50</sub> values 5-13 μM) [6,7]. Both enzymatic and crystal studies suggested that the mechanism of RNase H inhibition by DKA derivatives involves the sequestration of the divalent cofactor in the enzyme active site [6-8]. A second series of RNase H inhibitors are the *N*-acyl hydrazone derivatives among which is *N*-(4-*tert*-butylbenzoyl)-2-hydroxy-1-naphthaldehyde hydrazone (BBNH, Fig. 1) that has been reported to inhibit both HIV-1 RT-associated functions (IC<sub>50</sub> values 2-14 μM) [9]. More recently, the BBNH analogue (*E*)-3,4-dihydroxy-*N'*-((2-methoxynaphthalen-1-yl)methylene) benzohydrazide (DHBNH, Fig. 1) has been reported to selectively inhibit the HIV-1 RNase H function [10]. Crystal structure studies have shown that, differently from DKAs, DHBNH binds to a newly identified site comprised between the non-nucleoside RT inhibitors (NNRTI)-binding pocket and the polymerase active site [10]. At the best of our knowledge [5], these agents are among the most potent and selective anti-RNase H agents so far identified, so that, given the need to improve the anti-HIV therapeutic armamentarium with agents targeted at new viral sites, efforts aimed to identify new HIV-1 RNase H inhibitors are strictly required.

\*Address correspondence to this author at the Department of Applied Sciences in Biosystems, University of Cagliari, Cittadella Universitaria di Monserrato, SS554, I-09042 Monserrato, Italy; Tel: +39-0706754538; Fax: +39-0706754536; E-Mail: tramon@unica.it

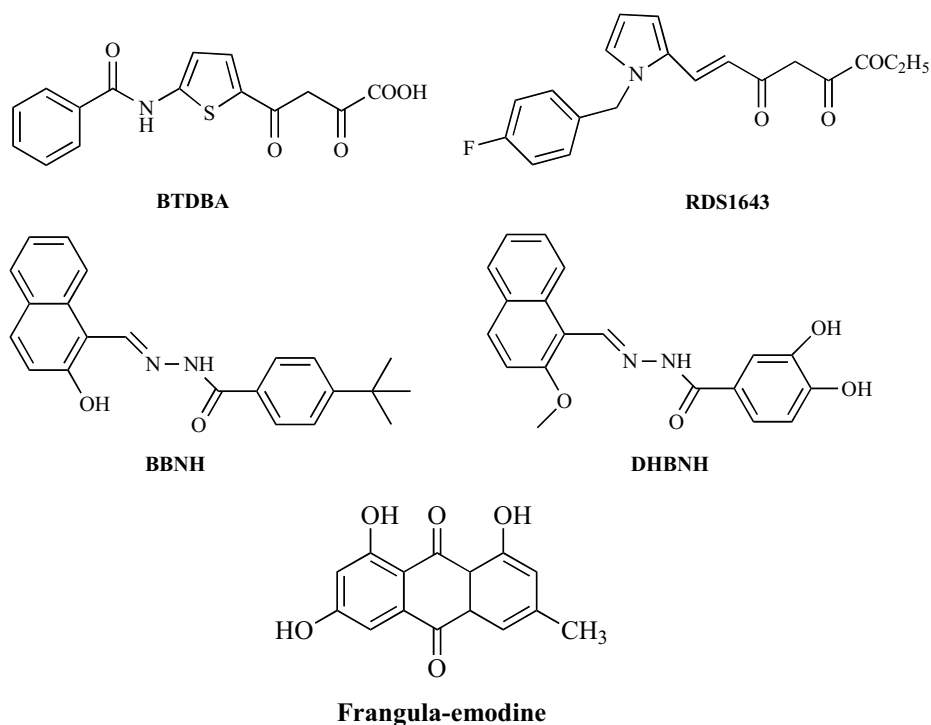


**Fig. (1).** Chemical structures of HIV-1 RNase H inhibitors.

Anthraquinones are common secondary metabolites occurring in bacteria, fungi, lichens, and higher plants where they are found in a large number of families [11]. Among the anthraquinone derivatives, 1,6,8-trihydroxy-3-methylantraquinone (frangula-emodine, Fig. 1) has been reported to be an active ingredient of various Chinese herbs [12], to have diverse biological properties including anti-microbial, anti-inflammatory, anti-proliferative, and anti-angiogenic effects [12,13], to inhibit the human protein kinase CK2 [14] and to have DNA intercalation ability [15-17]. Furthermore, frangula-emodin has been reported to inhibit, in cell-based assays, the human cytomegalovirus [18] and hepatitis B virus replication [19], and the Epstein-Barr virus activation [20]. Other anthraquinone derivatives, structurally related to frangula-emodin, have also been reported to inhibit the HIV-1 integrase activity in biochemical assays [21]. More recently, anthraquinones have been identified as potential HIV-1 integrase inhibitors through a dynamic pharmacophore model optimization [22].

Given all these considerations, in the search of new inhibitors of the HIV-1 RT-associated RNase H function we have synthesized a series of novel frangula-emodine analogues and have tested them for their effect on the HIV-1 RT-associated activities. In this report we have identified the frangula-emodine analogue 7-brom-6-O-phenacyl-1,8-dihydroxy-3-methylantraquinone (K67) which inhibits both HIV-1 RT-associated activities at low micromolar concentrations. Furthermore, we have characterized its mechanism of action and its interaction with the NNRTI nevirapine, demonstrating that it does not bind to the NNRTI binding site. Finally, we also have demonstrated that K67 mode of action differs from the one shown by DKA derivatives while it is

possibly compatible with the one shown by some hydrazone analogs.

## MATERIALS AND METHODS

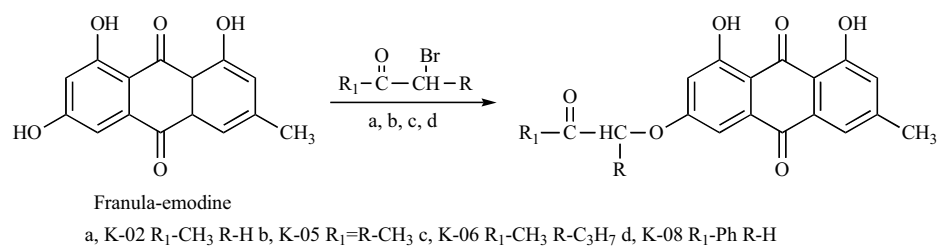
### Materials

P6HRT-prot plasmid was kindly provided by Dr. S. Le Grice (NCI at Frederick). [ $^3\text{H}$ ]-dGTP, activated calf thymus DNA and His-binding resin were obtained from GE Healthcare; [ $\gamma^{32}\text{P}$ ]-ATP was purchased by PerkinElmer; G-25 Sephadex quick spin column, T4 polynucleotide kinase and *E. coli* RNase H were from Roche. The p12 DNA oligonucleotide (5'-GTCTTTCTGCTC-3'), the tC5U RNA oligonucleotide (5'-CCCCUCUCAAAAACAGGAGCAGAAAGACAAG-3'), and the 12mer DNA oligonucleotide oligo(G) $_{12}$  was purchased by Operon. All buffer components and the other materials were obtained from Sigma-Aldrich.

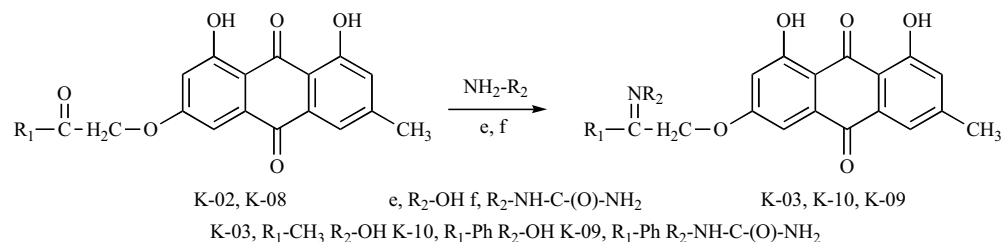
### Synthesis of Compounds

All solvents used were reagent grade and, when necessary, were purified and dried by standard methods. All reactions were monitored by thin layer chromatography (TLC) with Silufol plates. Developed plates were visualized by UV light. Melting points of the synthesized derivatives were determined on a Boetius apparatus. UV spectra were recorded on spectrometer UV/V is "Spectrometer Perkin-Elmer Lambda 35" in ethanol or acetonitrile ( $\lambda_{\text{max}}$ , nm). Infrared- (IR-) spectra were recorded on spectrometer "Nicolet 5700" (tablets of KBr, in  $\text{cm}^{-1}$ ). Mass-spectra (EI, 70 eV) were obtained on a "Finnigan MAT 8200" instrument.  $^1\text{H}$  NMR and  $^{13}\text{C}$  NMR spectra were recorded on a "Mercury-300" spectrometer at 300 MHz for  $^1\text{H}$  NMR and 75 MHz for  $^{13}\text{C}$  NMR, using HMDS as internal standard (chemical shifts in  $\delta$  values).

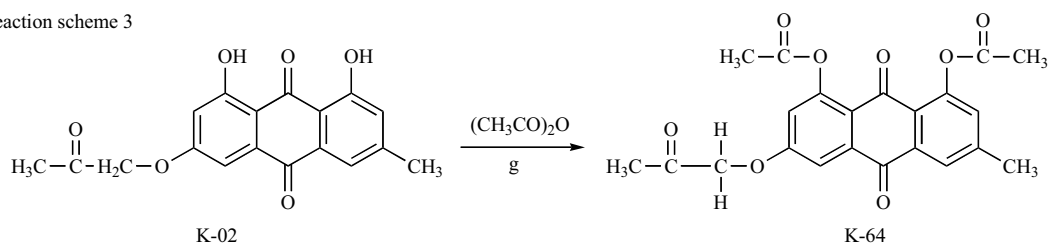
Reaction scheme 1



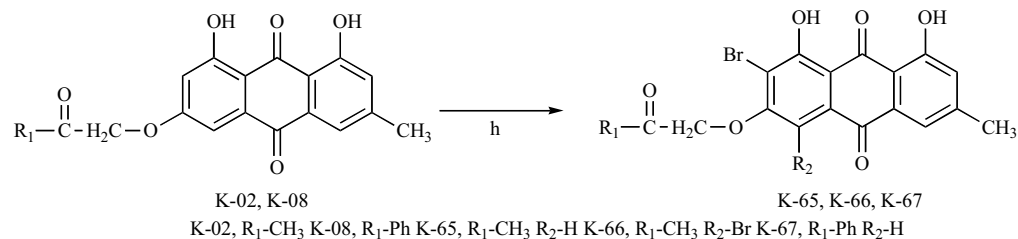
Reaction scheme 2



Reaction scheme 3

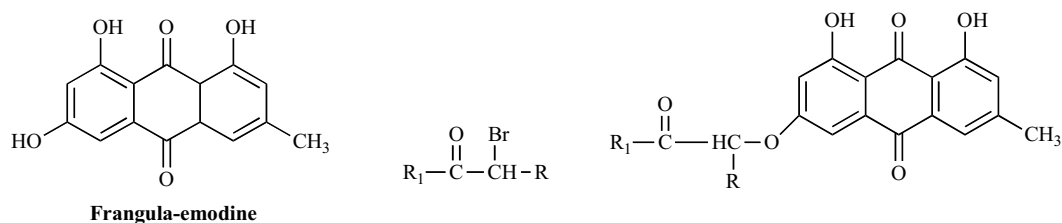


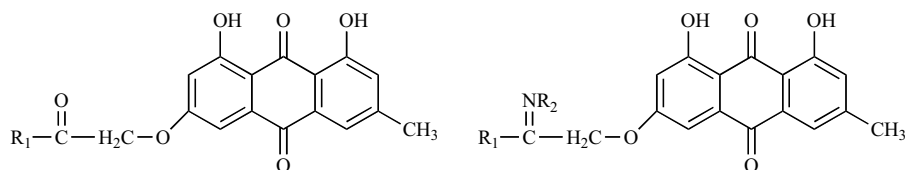
Reaction scheme 4

**Fig. (2).** Reaction schemes.**General Procedure for the Preparation of Compounds K02, K05, K06, K08 (Fig. 2, Scheme 1)**

In a three-necked flask at room temperature 2.7 g (0.01 mol) of frangula-emodine and (0.01 mol) of the appropriate  $\alpha$ -bromoketone [(a)  $\alpha$ -bromacetone, (b)  $\alpha$ -brommethyl-ethylketone, (c)  $\alpha$ -brommethyl-butylketone, (d)  $\omega$ -bromacetophenone] were dissolved in 100 ml of acetone and

mixed. Then, 1.38 g (0.01 mol) of K<sub>2</sub>CO<sub>3</sub> were added. The mixture was stirred, then heated at 55 °C. Hashing proceeded within 3-15 hours. The solvent was then removed and the residue was cooled to room temperature and poured in cold water with HCl. The formed precipitate was filtered, washed by water and dried. The crude product was purified by column chromatography.

**Scheme 1.**



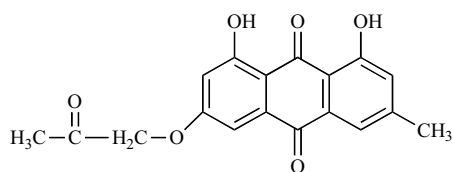
Scheme 2.

**Synthesis of K03 (Fig. 2, Scheme 2)**

In a three-necked flask 0.65 g (0.002 mol) of K02 were dissolved in 50 ml alcohol and hydroxylamine (e) (0.003 mol) and mixed. Then, NaOAc was added. After stirring, the reaction mixture was heated at 55 °C and hashing proceeded within 3-5 hours. Then the solvent was removed, the residue cooled to room temperature, and poured in cold water with HCl. The formed precipitate was filtered, washed by water and dried. The product of reaction K03 was purified by crystallization.

**Synthesis of K10 (Fig. 2, Scheme 2)**

In a three-necked flasks 0.78 g (0.002 mol) K-008 and hydroxylamine (e) (0.003 mol) were dissolved in 50 ml of alcohol and stirred. Then, NaOAc was added. After mixing,

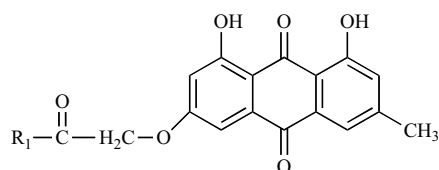


Scheme 3.

the reaction was heated at 55 °C and hashing proceeded within 3-5 hours. Then, the solvent was removed, the reaction mixture was cooled to room temperature, and a poured in cold water with HCl. The formed sediment was filtered, washed by water, and dried. The product of reaction K10 was purified by crystallization.

**Synthesis of K09 (Fig. 2, Scheme 2)**

In three-necked flask 0.78 g (0.01 M) of K-008 and semicarbazide (f) (0.003 mol) were dissolved in 50 ml of alcohol under stirring. Then, NaOAc was added. The reaction mixture was stirred and heated at 55 °C. Hashing proceeded within 3 hours. The solvent was removed and the reaction mixture was cooled to room temperature and a poured in cold water with HCl. The formed precipitate was filtered, washed by water, and dried. The product of reaction K09 was purified by crystallization.



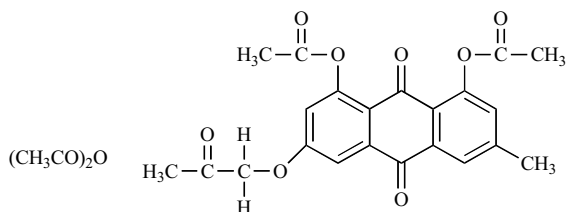
Scheme 4.

**Synthesis of K64 (Fig. 2, Scheme 3)**

To a solution of 0.65 g (0.002 mol) K02 in acetic anhydride (g) (50 ml) NaOAc were added. The reaction mixture was stirred and heated and refluxed for several hours, then cooled to room temperature and poured in cold water. The formed precipitate was filtered, washed by water and dried. The product of the reaction K64 was purified by crystallization.

**General Procedure for the Preparation of compounds K65-K66-K67 (Fig. 2, Scheme 4)**

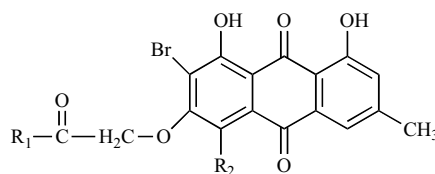
To a solution of K02 or K08 (0.002 mol) in a mixture of diethyl ether - dioxane (1:1) (50 ml) dioxane - dibromide (h) (0.002 mol for the synthesis of K65 and K67) or (0.004 mol



for the synthesis K66) were added. The reaction mixture was heated at 30-50 °C. Completion of the reaction was followed by TLC. The solvent was removed and the residue cooled to room temperature and poured out in cold water with HCl. The formed precipitate was filtered, washed by water, and dried.

**Compounds Analysis and their Spectral Data are Reported in the Supplementary Data Section****HIV-1 RT Purification**

Heterodimeric RT was expressed essentially as described [7] with few modifications. Briefly, *E. coli* strain M15 containing the P6HRT-prot plasmid were grown up to an OD<sub>600</sub> of 0.8 and induced with IPTG 1.7 mM for 5 hrs. Protein purification was carried out with a BioLogic LP (Biorad) with a Ni<sup>2+</sup>-sepharose chromatography. Cell pellets were resus-



pended in Lyses Buffer (20 mM Hepes pH 7.5, 0.5 M NaCl, 5 mM  $\beta$ -mercaptoethanol, 5 mM imidazole, 0.4 mg/mL lysozyme), incubated on ice for 20 min, sonicated and centrifuged at 30,000  $\times g$  for 1 hr. The supernatant was applied to a His-binding resin column and washed thoroughly with Wash Buffer (20 mM Hepes pH 7.5, 0.3 M NaCl, 5 mM  $\beta$ -mercaptoethanol, 60 mM imidazole, 10% glycerol). RT was gradient-eluted with Elute Buffer (Wash Buffer with 0.5 M imidazole), fractions were collected and enzyme activity was assessed; protein purity was checked by SDS-PAGE and found to be higher than 90%. Enzyme containing fractions were pooled, dialyzed against the Storage Buffer (50 mM Tris-HCl pH 7.0, 25 mM NaCl, 1 mM EDTA, 10% glycerol) and aliquots were stored at  $-80^{\circ}\text{C}$ .

#### **RNase H Polymerase-Independent Cleavage Assay**

When the Poly(dC)-[ $^3\text{H}$ ]Poly(rG) hybrid was used as reaction substrate the RNase H activity was measured as described [23]. Briefly, RNase H activity was measured in 50  $\mu\text{L}$  reaction volume containing 50 mM Tris HCl pH 7.8, 6 mM  $\text{MgCl}_2$ , 1 mM dithiothreitol (DTT), 80 mM KCl, 50 nM Poly(dC)-[ $^3\text{H}$ ]Poly(rG) and 3.8 nM RT. The reaction mixture was incubated for 1 hr at  $37^{\circ}\text{C}$ , 40  $\mu\text{L}$  aliquots were spotted on glass fiber filters (Whatman GF/A) and processed for determination of trichloroacetic acid-insoluble radioactivity [23]. When the *E. coli* RNase H activity was measured, the Poly(dC)-[ $^3\text{H}$ ]Poly(rG) hybrid was used as reaction substrate with the buffer conditions indicated by the manufacturer, and the trichloroacetic acid-insoluble radioactivity was determined as above. When the tC5U/p12 hybrid was used as reaction substrate the RNase H activity was measured as described [7] with the only exception that the reaction products were visualized and quantified by a Kodack CR system and a specifically developed software for quantitative analysis.

#### **DNA Polymerase Assay**

The RNA-dependent DNA polymerase (RDDP) activity of HIV-1 RT was measured as described [24] in 50  $\mu\text{L}$  volume containing 50 mM Tris-HCl pH 7.8, 80 mM KCl, 6 mM  $\text{MgCl}_2$ , 1 mM DTT, 2  $\mu\text{M}$  poly(rC)-oligo(dG) $_{12}$ , 10  $\mu\text{M}$  [ $^3\text{H}$ ]-dGTP (1 Ci  $\text{mmol}^{-1}$ ) and 40 nM HIV-1 RT. The DNA-dependent DNA polymerase (DDDP) activity was measured in 50  $\mu\text{L}$  volume containing the same buffers as above and 0.3 U/mL activated calf thymus DNA, 10  $\mu\text{M}$  each of dATP, dCTP and dGTP, and 10  $\mu\text{M}$  [ $^3\text{H}$ ]-TTP (1 Ci  $\text{mmol}^{-1}$ ) and 50 nM HIV-1 RT. For both RDDP and DDDP assays, the reaction mixtures were incubated for 1 hr at  $37^{\circ}\text{C}$ , 40  $\mu\text{L}$  aliquots were processed for trichloroacetic acid-insoluble radioactivity [24].

#### **Kinetic Studies**

The analysis of the kinetic of inhibition was performed according to Lineaweaver-Burke plots;  $v$  was expressed as fmoles/min,  $K_i$  was calculated by replotting the intercept values versus the inhibitor concentration using the Sigmaplot 9.0 software. The Yonetani-Theorell graphical method was performed as described [25]. The graphic isobologram method has been used as described [26]. The method consists of plotting on an arithmetic scale the amount of drug A and B that, alone and in various combinations, produces the same enzyme inhibition ( $\text{IC}_{50}$ ).

#### **DNA-Binding Assay**

The the DNA-binding ability was measured as described [16] with minor modifications. Briefly, the fluorescence was detected with a Perkin-Elmer LS-3 spectrofluorimeter in 3 mL volume containing 750 ng of calf thymus DNA, 10 mM Tris-HCl pH 8.0, 1 mM EDTA and 2  $\mu\text{M}$  of Hoechst 33342. The excitation wavelength was set at 346 nm and the emission wavelength at 460 nm.

#### **Cytotoxicity Assay**

K562 erythroleukemia cells were seeded at  $5 \times 10^4$  cell/ml into 96-well plates in growth medium RPMI1640 containing 10% fetal calf thymus serum (FCS), 100 U/mL penicillin G and 100  $\mu\text{g}/\text{mL}$  streptomycin in the absence or in the presence of different compound concentrations. All conditions were in duplicate. After a 4-days incubation at  $37^{\circ}\text{C}$ , cell viability was measured by the 3-(4,5-dimethylthiazol-2-yl)-2,5-diphenyl-tetrazolium bromide (MTT) method as described [27].

#### **HIV-1 Replication Assay**

Drug-mediated inhibition of virus-induced cytotoxicity was assayed in MT-2 cells as described [28] with minor modifications. Briefly, triplicate wells of 96-well plates containing  $1 \times 10^4$  MT-2 cells were infected with HIV-1 IIIB strain at a multiplicity of infection of 0.1. Serial dilutions of drug were added immediately after infection. Cell viability was quantified 5 days after infection with the MTT-dye reduction method [29].

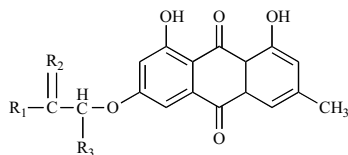
## **RESULTS**

#### **Identification of K67**

Both HIV-1 RNase H and integrase catalyze the phosphoryl transfer through nucleophilic substitution reaction on phosphate esters, belong to the superfamily of polynucleotidyl transferases and share striking structural and functional homologies [30,31]. In fact, DKA derivatives, originally designed for anti-integrase activity, have been found to inhibit also the viral RNase H function [6,7]. In initial screenings aimed to identify new HIV-1 integrase agents, some anthraquinone derivatives have been reported to inhibit the integrase in biochemical assays [21]. More recently, a dynamic pharmacopore model optimization has allowed to recognize that anthraquinone derivatives interact with the integrase protein [22]. Among the anthraquinone analogues tested, the anthraquinone frangula-emodine was not able to inhibit the HIV-1 integrase in biochemical assays [21], however at our best knowledge, no information was available on the ability of this anthraquinone to interact with the HIV-1 RT functions. Therefore, within our program aimed to identify new HIV-1 RNase H inhibitors we assayed frangula-emodine for its effect on the HIV-1 RT-associated polymerase-independent RNase H activity in biochemical assays and found that it inhibited this enzyme function with an  $\text{IC}_{50}$  value of 76  $\mu\text{M}$  (Table 1).

Based on this initial observation, we synthesized a series of  $\beta$ -acetyl- and  $\beta$ -phenacyl-frangula-emodine analogues, we tested them for their ability to inhibit the HIV-1 RT-associated polymerase-independent RNase H activity in biochemical assays and found that they are less active than

**Table 1. Effect of  $\beta$ -acetyl- and  $\beta$ -phenacyl-frangula-emodine Derivatives on HIV-1RNase H Activity. Cleavage Reactions and Cytotoxicity Evaluations were Conducted as Described in the “Materials and Methods” Section. Values Represent the Mean and S.D. of at Least Three Independent Experiments**



Compounds	R <sub>1</sub>	R <sub>2</sub>	R <sub>3</sub>	<sup>a</sup> IC <sub>50</sub> (μM) HIV-1 RNase H	<sup>b</sup> CC <sub>50</sub> (μM) K562
Frangula-emodine				75 ± 7	35 ± 5
K02	CH <sub>3</sub>	O	H	> 100 ( <sup>c</sup> 56%)	> 100 ( <sup>d</sup> 69%)
K03	CH <sub>3</sub>	>N-OH	H	> 100 (73%)	33 ± 6
K05	CH <sub>3</sub>	O	CH <sub>3</sub>	> 100 (77%)	> 100 (71%)
K06	CH <sub>3</sub>	O	CH <sub>3</sub> -CH <sub>2</sub> -CH <sub>2</sub> -	> 100 (98%)	> 100 (66%)
K08	Ph	O	H	> 100 (75%)	> 100 (98%)
K10	Ph	>N-OH	H	> 100 (85%)	> 100 (86%)
K09	Ph	>N-NH-C(O)-NH <sub>2</sub>	H	> 100 (90%)	100 ± 9

<sup>a</sup>Compound concentration required to reduce the HIV-1 RNase H activity by 50%.

<sup>b</sup>Compound concentration required to reduce the K562 cell multiplication by 50%.

<sup>c</sup>Percentage of enzyme activity observed in the presence of the higher compound concentration tested (100 μM).

<sup>d</sup>Percentage of cell multiplication observed in the presence of the higher compound concentration tested (100 μM).

frangula-emodine at the higher compound concentration tested (Table 1). A second series of frangula-emodine analogues was then synthesized. The diacetate derivative of K02, K64, which has two acetate substituents in position 1 and 8 of the anthraquinone structure and an acetyl group in position 6 was inactive on the RNase H (Table 2). Differently, when the acetate substituents were replaced by the standard frangula-emodine hydroxyls and a bromine atom was introduced in position 7, K65 inhibited the HIV-1 RNase H activity with an IC<sub>50</sub> value of 56 μM and was not cytotoxic on K562 cells (Table 2). The further introduction of a second bromine atom in position 5, which led to the K66, did not increase the potency of RNase H inhibition. However, when the acetyl group of compound K65 was replaced with a phenacyl group, the resulting compound, K67, inhibited the HIV-1 RT-associated activity with an IC<sub>50</sub> value of 14 μM (Fig. 3A).

Since it has been reported that the HIV-1 RNase H activity could be influenced by the sequence of the RNA:DNA template utilized in the biochemical assay [32], we also used a different, previously described [6], RNA:DNA hybrid substrate to assess the K67 effect on the HIV-1 RNase H function. Results showed that, also with this substrate, K67 inhibited the HIV-1 RT-associated polymerase-independent RNase H function with an IC<sub>50</sub> value of 16 μM (Fig. 3B) without affecting the RNase H cleavage pattern. The DKA derivative RDS1643 was used as control and showed an IC<sub>50</sub> value of 12 μM.

### K67 selectivity

In order to explore the K67 selectivity, we assayed the effect of the anthraquinone analogues which were active on

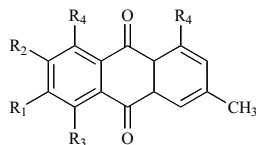
the HIV-1 RNase H function also on other enzymes. Firstly, we assessed their activity on the HIV-1 RT-associated polymerase function, using both RNA and DNA templates as reaction substrate. In biochemical assays, K67 inhibited both HIV-1 RT RDDP and DDDP activities with a 3.7 fold difference in potency of inhibition (Table 3), which is comparable to the template-dependent inhibition potency shown, in biochemical assays, by BBNH [9] and other NNRTIs [24]. Secondly, in order to avoid the possibility that K67 could act non specifically on the HIV-1 RT, we assayed its effect on the hepatitis C virus RNA-dependent RNA polymerase (RdRp) activity and found that it was inactive on this enzyme (Table 3). Thirdly, since it has been reported that BBNH inhibited also the *E. coli* RNase H activity, we tested K67 also on this bacterial enzyme (Table 3). Results showed that, similarly to BBNH, all compounds that inhibited the viral RNase H function also inhibited the bacterial enzyme. Next, we assessed the ability of K67 and the other frangula-emodine analogues to inhibit the HIV-1 IIIB strain replication in MT2 cells and found that they were all inactive on the viral replication (Table 3). Noteworthy, we found that frangula-emodin, K65 and K66 were cytotoxic on MT2 cells, while K67 was not cytotoxic. Possibly, the lack of antiviral effect of K67 is due to a reduced cell uptake.

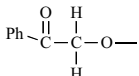
### K67 DNA-binding ability

It has been reported that frangula-emodine induces genotoxicity in replicating cells by binding non-covalently to dsDNA [15-17]. Since the reaction substrates used in our biochemical assays were double stranded nucleic acids (either RNA:DNA or DNA:DNA) we asked whether the observed enzyme inhibition by K67, frangula-emodine and the

**Table 2. Effect of Different Frangula-emodine Derivatives on HIV-1 RNase H Activity**

Cleavage Reactions and Cytotoxicity Evaluations were Conducted as Described in the “Materials and Methods” Section. Values Represent the Mean and S.D. of at Least Three Independent Experiments



Compounds	R <sub>1</sub>	R <sub>2</sub>	R <sub>3</sub>	R <sub>4</sub>	<sup>a</sup> IC <sub>50</sub> (μM) HIV-1 RNase H	<sup>b</sup> CC <sub>50</sub> (μM) K562
K64	OCH <sub>2</sub> COCH <sub>3</sub>	H	H	OCOCH <sub>3</sub>	> 100 ( <sup>c</sup> 85%)	59 ± 9
K65	OCH <sub>2</sub> COCH <sub>3</sub>	Br	H	OH	56 ± 7	> 100 ( <sup>d</sup> 95%)
K66	OCH <sub>2</sub> COCH <sub>3</sub>	Br	Br	OH	51 ± 6	> 100 (100%)
K67		Br	H	OH	14 ± 4	> 100 (100%)

<sup>a</sup>Compound concentration required to reduce the HIV-1 RNase H activity by 50%.

<sup>b</sup>Compound concentration required to reduce the K562 cell multiplication by 50%.

<sup>c</sup>Percentage of enzyme activity observed in the presence of the higher compound concentration tested (100 μM).

<sup>d</sup>Percentage of cell multiplication observed in the presence of the higher compound concentration tested (100 μM).

other analogues could be due to a non specific binding of the compounds to the nucleic acid substrate that could, in turn, interfere with the enzyme activity. To exclude this possibility we evaluated frangula-emodine and K67 abilities to bind to calf thymus DNA in solution. The method was based on the elevated fluorescence of Hoechst 33342 when it binds non-covalently to DNA. The addition of other DNA-binding compounds causes a reduction of this fluorescence due to a competition for the DNA binding. The anti-tumor drug doxorubicin was used as control. Results showed that doxorubicin competed with Hoechst 33342 for DNA-binding, inhibiting its fluorescent signal with an IC<sub>50</sub> value of 6.0 μM (Fig. 4A). Accordingly with previous observations [16], frangula-emo-

dine inhibited the Hoechst 33342 fluorescent signal showing an IC<sub>50</sub> value of ~ 60 μM (Fig. 4B). On the contrary, K67 did not shown any inhibition of the Hoechst 33342 fluorescent signal at 96 μM concentration (Fig. 4C). Similarly to K67, also the other frangula-emodine analogues active on the HIV-1 RT functions were not able to bind non-covalently to DNA (data not shown). Noteworthy, neither K67 nor other frangula-emodine derivatives affected Hoechst 33342 fluorescence in the absence of DNA (data not shown). Overall, these results suggest that the inhibition of the HIV-1 RT functions by K67 is not due to a non-covalent binding to the nucleic acids used as enzyme substrates.

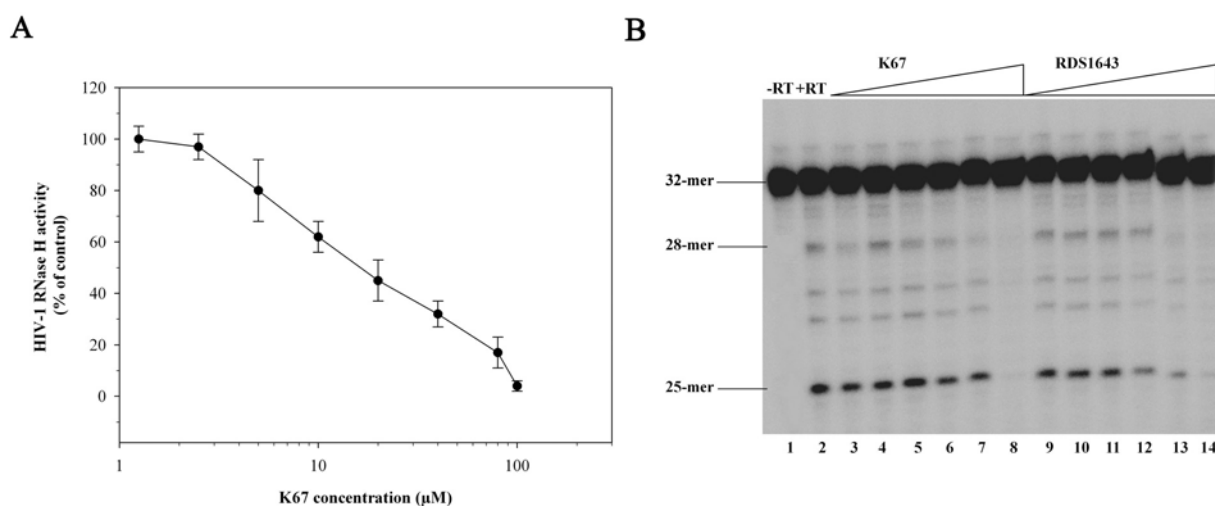


**Fig. (3).** Inhibition of the polymerase-independent HIV-1 RNase H activity by K67. (A), reactions contained Poly(dC)-[<sup>3</sup>H]Poly(rG) as reaction substrate and were carried out as described under “Materials and Methods”. Data represent mean values and standard deviations from three independent determinations. (B), PAGE analysis were carried out as described under “Materials and Methods”. Four major bands were resolved as reaction products, each of them coming from a single cleavage event of the 32<sup>mer</sup> substrate. Lane 1 without RT; lane 2 plus RT, lanes 3-8 plus RT and K67 (0.3, 1, 3, 11, 33, 100 μM); lanes 9-14 plus RT and RDS 1634 (0.3, 1, 3, 11, 33, 100 μM).

**Table 3. Selectivity of Action of Frangula-Emodine Analogues**

Enzyme Reactions and Viral Evaluations were Conducted as Described in the “Materials and Methods” Section. Values Represent the Mean and S.D. of at Least Three Independent Experiments

Compounds	<sup>a</sup> IC <sub>50</sub> (μM)				<sup>b</sup> EC <sub>50</sub> (μM)	<sup>c</sup> CC <sub>50</sub> (μM)
	HIV-1 RDDP	HIV-1 DDDP	HCV RdRp	<i>E. coli</i> RNase H	HIV-1	MT-2
Frangula-emodine	45 ± 6	76 ± 9	<sup>d</sup> ND	ND	> 70	70
K65	22 ± 4	63 ± 7	> 100	16 ± 4	> 30	30
K66	17 ± 5	60 ± 8	> 100	6.8 ± 7	> 18	18
K67	35 ± 3	52 ± 7	> 100	17.5 ± 4	> 100	> 100
Nevirapine	0.21 ± 0.03	ND	> 100	> 100	ND	ND

<sup>a</sup>Compound concentration required to reduce enzyme activities by 50%.

<sup>b</sup>Compound concentration required to reduce the HIV-1 induced cytopathic effect in MT2 cells by 50%.

<sup>c</sup>Compound concentration required to reduce the MT-2 cell multiplication by 50%.

<sup>d</sup>Not done.

### K67 Time-Dependence Inhibition

In order to gain a closer insight into the interaction between the HIV-1 RT and K67, we evaluated whether this

interaction could be affected by the time of addition of the reaction mixture components. Results showed that the HIV-1 RNase H inhibition by K67 was identical when *i*) the compound was preincubated with the enzyme in the absence of

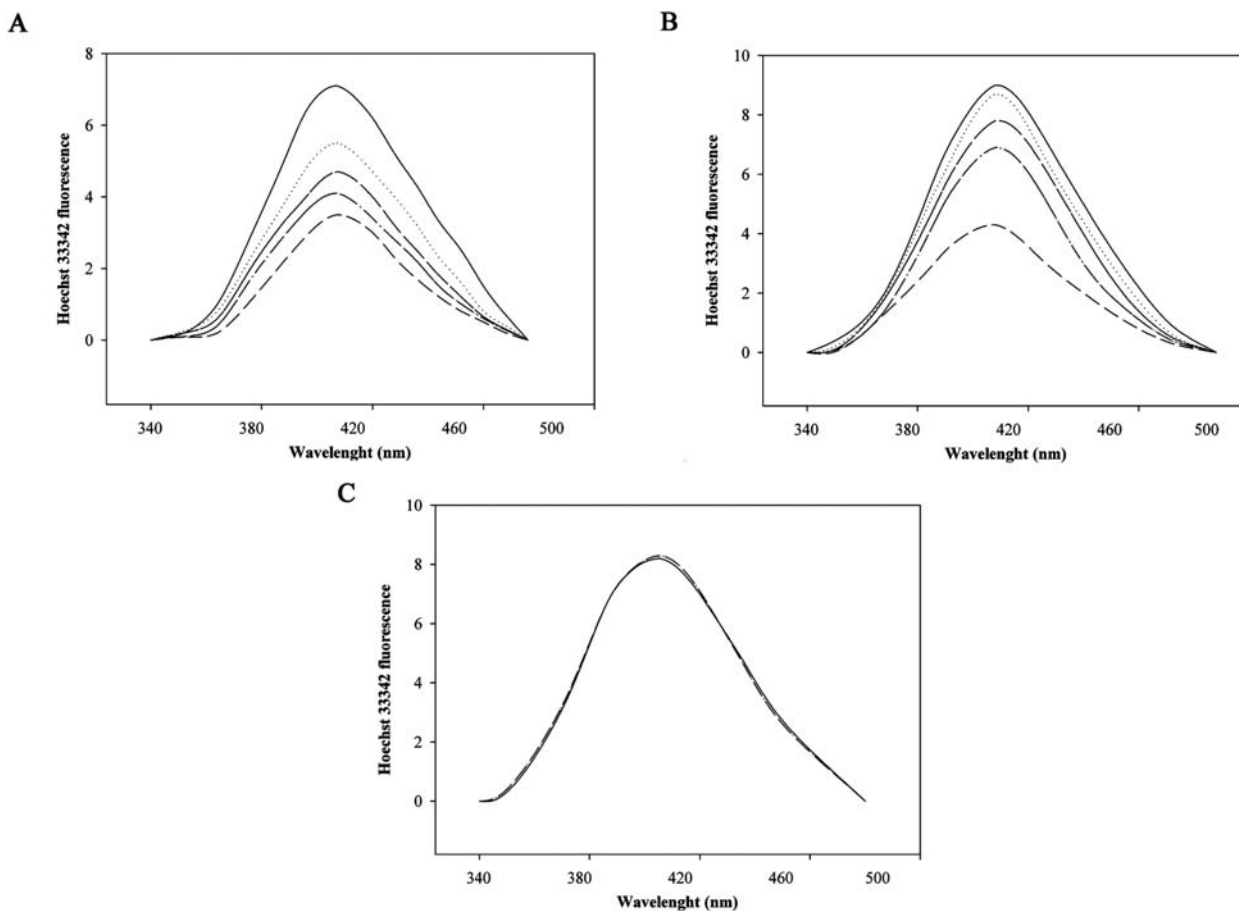


**Fig. (4).** Interference with Hoechst 33342 non-covalent binding to DNA. Reactions were carried out as described under “Experimental Procedures”. (A), Effects on Hoechst 33342 binding to dsDNA by Doxorubicin (0; 1 μM; 2 μM; 4 μM; 8 μM). (B), Effects on Hoechst 33342 binding to dsDNA by frangula-emodine (0; 8 μM; 16 μM; 32 μM; 64 μM). (C), Effects on Hoechst 33342 binding to dsDNA by K67(0; 96 μM).



**Table 4. K67 time-Dependence Inhibition of the HIV-1 RNase H Activity**

Enzyme Reactions were Conducted as Described in the “Materials and Methods” Section. Values Represent the Mean and S.D. of at Least Three Independent Experiments

Experimental Condition	<sup>a</sup> IC <sub>50</sub> (μM)
K67 + RT → 10' preincubation → + substrate → reaction incubation	17 ± 5
K67 + RT + substrate → reaction incubation	14 ± 4
RT + substrate → 10' preincubation → + K67 → reaction incubation	18 ± 2

<sup>a</sup>Compound concentration required to reduce HIV-1 RT RNase H activity by 50%.

the substrate; *ii*) the compound and all the components of the reaction mixture were incubated at the same time (the standard experimental condition); *iii*) the compound was added to the reaction mixture after the enzyme had been preincubated with the substrate to allow the formation of the RT/substrate complex (Table 4).

### Kinetics of HIV-1 RT Polymerase-independent RNase H Inhibition by K67

The hydrolysis of the Poly(dC)-[<sup>3</sup>H]Poly(rG) hybrid substrate by the HIV-1 RNase H is a processive reaction which can be monitored according to the Michaelis-Menten kinetic assumptions. In this system, the  $K_m$  and  $k_{cat}$  values were of 28 nM and 0.66 sec<sup>-1</sup>, respectively. Kinetics of inhibition studies demonstrated that K67 is a non competitive inhibitor of the polymerase-independent RNase H activity, with a  $K_i$  value of 10 μM (Fig. 5).

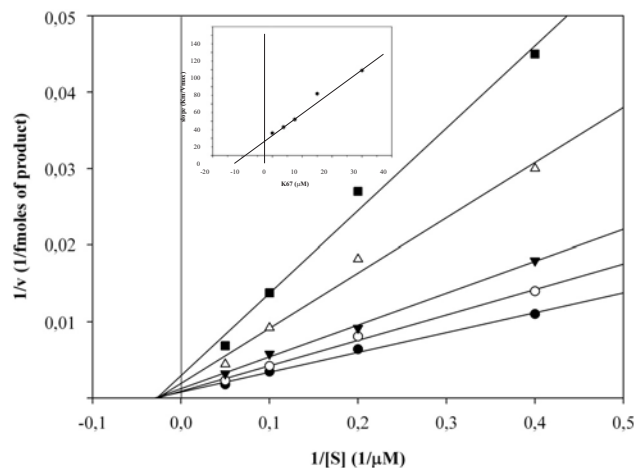


**Fig. (5).** Lineweaver-Burk plot of the inhibition of the polymerase-independent HIV-1 RNase H activity by K67. Reactions were performed as described under “Materials and Methods”. HIV-1 RT was incubated in the absence (○) or in the presence of 3.75 μM (○), 7.5 μM (▼), 15 μM (▲) or 30 μM (■) K67. Inset, replot of the line slopes obtained in the Lineweaver-Burk plot against the K67 concentration to calculate the  $K_i$  value.

### Interaction of K67 and nevirapine on the HIV-1 RT RDDP activity

It has been observed that combinations of NNRTI and DKA derivatives are additive on the HIV-1 RDDP activity

(i.e. the enzyme inhibition effect obtained by a NNRTI alone is the same that the effect obtained in the presence of both NNRTI and DKA derivative) [6,7]. Furthermore, the observation that K67 inhibits both enzyme activities suggested that it may not bind with the NNRTI binding site. Therefore, it was of interest to ascertain which interaction takes place between K67 and the NNRTI nevirapine. In order to investigate this interaction, we used the Yonetani-Theorell model, as revised by Yonetani [25], that allows to determine whether two inhibitors of a certain enzyme compete for the same binding site or act on two non overlapping binding sites and that was already used to dissect the effect of the interaction between RNase H and RDDP inhibitors [33]. In this revised model, the plot of the reaction velocity reverse ( $1/v$ ) observed in the presence of different concentrations of the first inhibitor, in the absence or in the contemporaneous presence of the second inhibitor, leads to a series of lines which are parallel if the two inhibitors compete for the same binding site, whereas they intersect if the inhibitors bind to different enzyme sites [25]. Therefore, the HIV-1 RT RDDP activity was measured in the presence of increasing concentrations of both K67 and nevirapine and analyzed with the Yonetani-Theorell plot (Fig. 6A). Results showed that both slope and intercepts of the plots of  $1/v$  versus K67 concentration increased as linear function of nevirapine, indicating that the two compounds do not bind to overlapping sites.

The same results, obtained in the presence of increasing concentrations of both K67 and nevirapine, were also analyzed with the graphic isobologram method which allows to evaluate the combination effectiveness of two inhibitors. This analysis showed that the effects of K67 and nevirapine on the HIV-1 RT RDDP activity are additive (Fig. 6B).

### Interaction of K67 and nevirapine on the HIV-1 RT polymerase-independent RNase H activity

It has been shown that there is a significant interdomain communication between the NNRTI binding site domain and the RNase H domain. In fact, in enzymatic assays, TIBO was reported to activate the HIV-1 polymerase-independent RNase H activity [34] and nevirapine was reported also to alter its cleavage specificity [35]. More recently, an efavirenz analog was shown to enhance the RNase H cleavage in a template-dependent manner and to decrease the HIV-1 RNase H inhibition by BTDBA [33]. Therefore, it was of interest to assess the effect of the interaction of the K67 and nevirapine also on the HIV-1 RNase H activity.

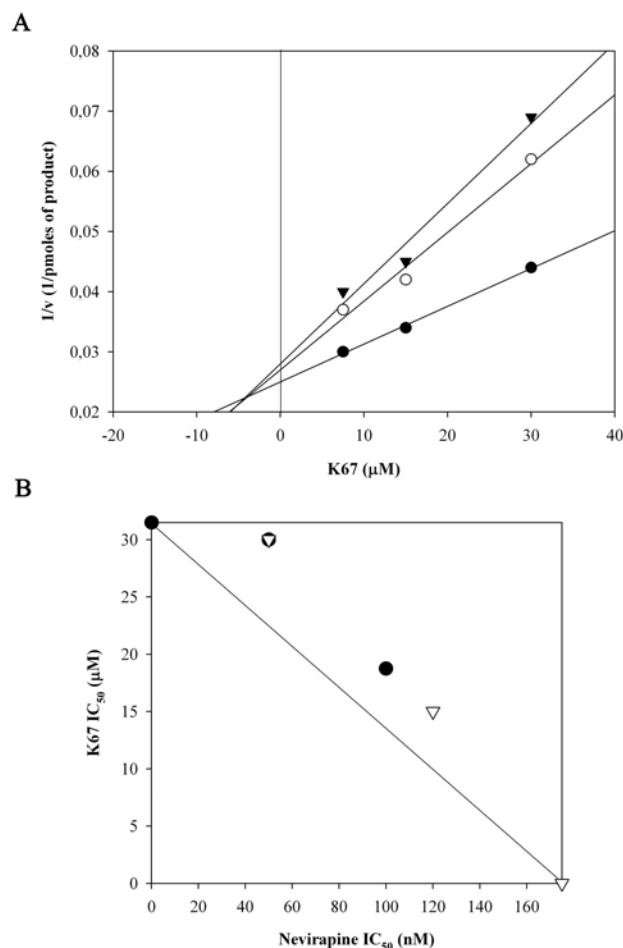


**Fig. (6).** Interaction of K67 and nevirapine on the HIV-1 RDDP activity. Reactions were performed as described under “Materials and Methods”. (A), Yonetani-Theorell plot of the combination of K67 and nevirapine on the HIV-1 RDDP activity. HIV-1 RT was incubated in the presence of different concentrations of K67 and in the absence (○) or in the presence of 50 nM (○) or 100 nM (▼) nevirapine. (B), Isobologram of the combination of K67 and nevirapine on the HIV-1 RT-associated RDDP activity. HIV-1 RT was incubated in the presence of increasing concentrations of K67 and nevirapine. The IC<sub>50</sub> values of K67 (○) obtained in the presence of different concentrations of nevirapine and the IC<sub>50</sub> values nevirapine (△) obtained in the presence of different concentrations of K67 are shown.

Firstly, in order to verify that, in our assay conditions, nevirapine was able to increase the HIV-1 polymerase-independent RNase H activity we measured the HIV RNase H kinetics in the presence of different nevirapine concentrations (Fig. 7A). Results showed that the catalytic constant,  $k_{cat}$ , increased from 0.74 min<sup>-1</sup> (no nevirapine) to 0.91, 1.37, 1.65 min<sup>-1</sup>, in the presence of 1, 10 and 100 μM nevirapine, respectively. However, given the parallel  $K_m$  value enhancement, the RNase H catalytic efficiency, as measured by the  $k_{cat}/K_m$  ratio, did not vary.

Then, it was of interest to apply the Yonetani-Theorell graphical method to confirm what was observed in the case of the HIV-1 RDDP inhibition. For this purpose we assayed the HIV-1 RT-associated RNase H activity in the presence of

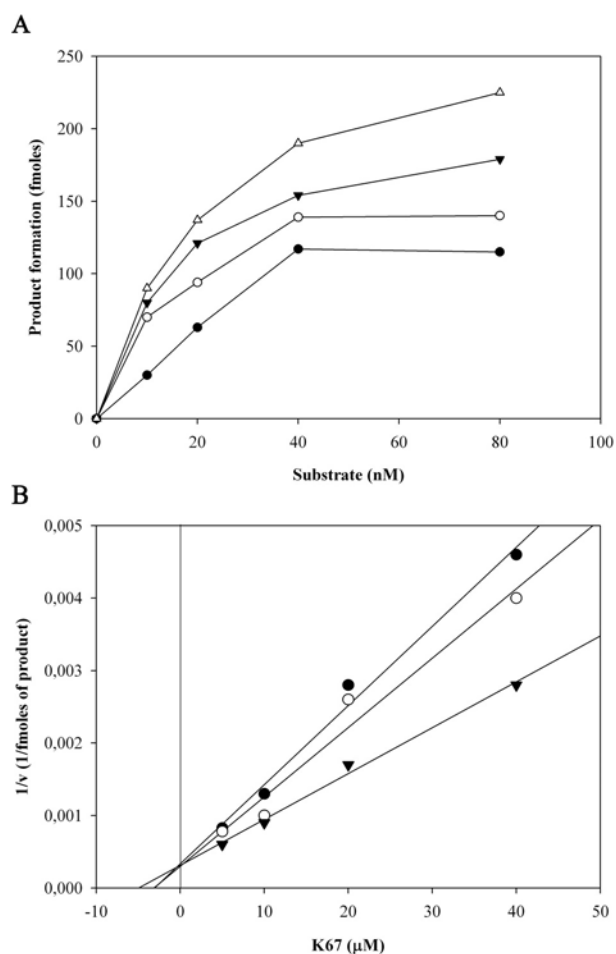


**Fig. (7).** Interaction of K67 and nevirapine on the polymerase-independent HIV-1 RNase H activity. Reactions were performed as described under “Materials and Methods”. (A), Kinetics of the nevirapine effect on the HIV-1 RT-associated RNase H activity. HIV-1 RT was incubated in the absence (○) or in the presence of 1 μM (○), 10 μM (▼), 100 μM (△) nevirapine. (B), Yonetani-Theorell plot of the combination of K67 and nevirapine on the HIV-1 RT-associated RNase H activity. HIV-1 RT was incubated in the presence of different concentrations of K67 and in the absence (○) or in the presence of 1 μM (○) or 10 μM (▼) nevirapine.

a combination of increasing concentrations of K67 and nevirapine and plotted the results according to the Yonetani-Theorell method. Results showed that the slope of the plots of  $1/v$  versus K67 concentration decreased at increasing nevirapine concentrations, confirming that the two compounds do not bind to overlapping sites (Fig. 7B). Furthermore, despite the increase in the HIV-1 RNase H activity induced by nevirapine, the K67 IC<sub>50</sub> values did not vary significantly at increasing nevirapine concentrations (IC<sub>50</sub> values were 12, 14 and 18 μM in the presence of 0, 1 and 10 μM nevirapine, respectively).

## DISCUSSION

In the search of new HIV-1 RNase H inhibitors, we considered that anthraquinones analogues were reported to interact with the structurally related HIV-1 integrase [21,22]. In the present report, we demonstrated that frangula-emodine

and a series of newly synthesized anthraquinone derivatives inhibited both HIV-1 RT-associated activities at micromolar concentrations showing a 2.5-fold selectivity for the HIV-1 RT RNase H function versus its polymerase function. Structure activity relationship studies revealed that the introduction of several substituents in position 6 of the anthraquinone structure reduced the HIV-1 RT inhibition shown by frangula-emodin. Conversely, the introduction of a bromine atom in position 7 led to a compound, K65, which inhibited the HIV-1 RNase H function at a concentration comparable to the one shown by frangula-emodin, and the substitution of its acetyl group with the bulkier phenacyl group led to the identification of K67, the most potent analogue of this series.

The mechanism of action studies performed on K67 *i)* excluded the possibility that it could intercalate in the reaction substrate nucleic acid (and that it could inhibit the enzyme catalysis non-specifically); *ii)* revealed that K67 inhibits the HIV-1 RT independently by the time of its addition to the reaction mixture; *iii)* showed that K67 is a non-competitive inhibitor of the HIV-1 RNase H function.

Since a major class of RNase H inhibitors identified so far are the DKA derivatives which, similarly to K67, are non-competitive inhibitors and were originally identified in HIV-1 integrase screening programs, we also investigated whether K67 could interact with the HIV-1 RT with a mechanism of action involving the sequestration of the  $Mg^{2+}$  divalent cofactor at the RNase H active site, as it was proposed for BTDBA and RDS1643 [6-8]. Given that, in a previous report, it was shown that the presence of  $Mg^{2+}$  determined a shift in the RDS1643 UV-visible spectrum [7] we investigated the possibility that K67 could chelate the  $Mg^{2+}$  through the observation of changes in the K67 UV-visible spectrum in the absence and in the presence of  $Mg^{2+}$ . The lack of any change in the K67 UV-visible spectrum at increasing  $Mg^{2+}$  concentrations (Fig. 8) seems to exclude the possibility that K67 chelates the divalent RT cofactor and suggests that it inhibits the RT catalysis with a mechanism of action different from the one shown by DKA derivatives.

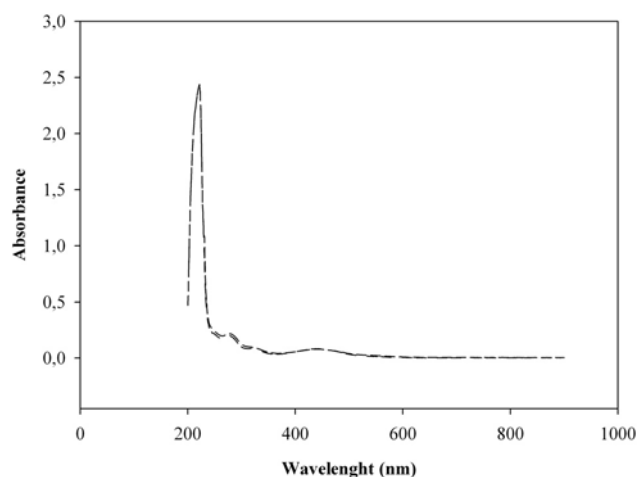


**Fig. (8).** Lack of  $Mg^{2+}$  chelation by K67. The K67 spectrum was determined with a Amersham Ultraspec spectrophotometer in the absence (short-short line) or in presence of 6 mM  $MgCl_2$  (short-dashed line).

The observation that K67 inhibited also the HIV-1 RT RDDP function led to the hypothesis that K67 might interact with the NNRTI binding site. However, firstly, it is important to note that no NNRTI has ever been reported to inhibit also the HIV-1 RT-associated RNase H activity but, on the contrary, they have been reported to increase its activity [33-35]. Secondly, the Yonetani-Theorell analysis of the interaction between nevirapine and K67 on both HIV-1 RT RDDP and RNase H functions clearly demonstrated that the two compounds bind to two non overlapping sites. Therefore, even in the absence of X-ray data, we can reasonably conclude K67 does not interact to the NNRTI binding site.

It is worth to note that other HIV-1 RNase H inhibitors such as naphthalenesulfonic acid derivatives [36], BBNH [9], quinones [37] were reported to inhibit both HIV-1 RT-associated polymerase activities. Furthermore, recently, the hydrazone derivative DHBNH was shown to inhibit the HIV-1 RNase H function non-competitively, to be equally effective on the RNase H function in the presence or in the absence of nevirapine, and to bind to a site which is between the NNRTI binding site and the polymerase active site and not in the vicinity of the RNase H binding site [10]. In addition, DHBNH analogues with a bulkier group in the *para* position of the DHBNH benzoyl ring were reported to be equally active on both RT-associated functions, showing that compounds interacting with this newly identified binding site can affect both RNase H and RDDP RT functions [10].

Overall, these results demonstrated that K67 is a new HIV-1 RNase H inhibitor which acts with a mechanism of action that is different from the one shown by the DKA derivatives while it is possibly compatible with the mechanism of action shown by DHBNH, even though more detailed X-ray studies would be needed to confirm this hypothesis. K67 was not able to inhibit the viral replication in cell-based assays, possibly due to the lack of cellular uptake, and further studies are needed to obtain more potent K67 derivatives. Finally, these results confirm the structural homologies between the HIV-1 integrase and RNase H enzymes and suggest that this similarity should be further explored in order to develop new anti-HIV agents.

## ACKNOWLEDGMENTS

This work was supported by EC-INTAS grant n. 04-82-7146, by Fondazione Banco di Sardegna n. 2008.0168 and by NIAID, NIH, grant n. AI-38204. Yung-Chi Cheng is a fellow of the National Foundation for Cancer Research.

## ABBREVIATIONS

- |          |   |  |
|----------|---|--|
| BBNH     | = | <i>N</i> -(4- <i>tert</i> -butylbenzoyl)-2-hydroxy-1-naphthaldehyde hydrazone              |
| BTDBA    | = | 4-[5-(benzo-ylamino)thien-2-yl]-2,4-dioxobutanoic acid                                     |
| DDDP DNA | = | Dependent DNA polymerase   |
| DKA      | = | Diketo acid  |
| DHBNH    | = | ( <i>E</i> )-3,4-dihydroxy- <i>N'</i> -((2-methoxynaphthalen-1-yl)methylene)benzohydrazide |

frangula-emodin	=	1,6,8-trihydroxy-3-methylanthraquinone
HIV-1	=	Human Immunodeficiency type 1
K02	=	6-O-(propan-2'-on)-1,8-dihydroxy-3-methylanthraquinone
K03	=	Oxime-6-O-(propan-2'-on)-1,8-dihydroxy-3-methylanthraquinone
K05	=	6-O-(1'-methy-propan-2'-on)-1,8-dihydroxy-3-methylanthraquinone
K06	=	6-O-(1'-propyl-propan-2'-on)-1,8-dihydroxy-3-methylanthraquinone
K08	=	6-O-phenacyl-1,8-dihydroxy-3-methylanthraquinone
K09	=	Semicarbazone-6-O-phenacyl-1,8-dihydroxy-3-methylanthraquinone
K10	=	Oxime-6-O-phenacyl-1,8-dihydroxy-3-methylanthraquinone
K64	=	6-O-(propan-2'-on)-1,8-diacetoxy-3-methylanthraquinone
K65	=	7-brom-6-O-(propan-2'-on)-1,8-dihydroxy-3-methylanthraquinone
K66	=	5,7-dibrom-6-O-(propan-2'-on)-1,8-dihydroxy-3-methylanthraquinone
K67	=	7-brom-6-O-phenacyl-1,8-dihydroxy-3-methylanthraquinone
RDS 1643	=	6-[1-(4-fluorophenyl)methyl-1 <i>H</i> -pyrrol-2-yl)]-2,4-dioxo-5-hexenoic acid ethyl ester
NNRTI	=	Non-nucleoside reverse transcriptase inhibitor
RDDP	=	RNA-dependent DNA polymerase
RNase H	=	Ribonuclease H
RT	=	Reverse transcriptase

## REFERENCES

- Arts, E.J.; Le Grice, S.F.J. Interaction of retroviral reverse transcriptase with template-primer duplexes during replication. *Progr. Nucl. Acid Res. Mol. Biol.*, **1998**, *58*, 341-393.
- Hughes, S.H.; Arnold, E.; Hostomsky Z. *RNase H of Retroviral Reverse Transcriptases*, in *Ribonucleases H*. Crouch, R.J.; Toulmé J.J., Ed.: Les Editions INSERM: Paris, France, **1998**, pp.195-224.
- Klarmann, G.J.; Hawkins, M.E.; Le Grice, S.T.J. Uncovering the complexities of retroviral ribonuclease H reveals its potential as a therapeutic target. *AIDS Rev.*, **2002**, *4*, 183-194.
- Tisdale, M.; Schulze, T.; Larder, B.A.; Moelling, K. Mutations within the RNase H domain of human immunodeficiency virus type 1 reverse transcriptase abolish virus infectivity. *J. Gen. Virol.*, **1991**, *72*, 59-66.
- Tramontano, E. HIV-1 RNase H: recent progress in an exciting, yet little explored, drug target. *Mini-Rev. Med. Chem.*, **2006**, *6*, 727-737.
- Shaw-Reid, C.A.; Munshi, V.; Graham, P.; Wolfe, A.; Witmer, M.; Danzeisen, S.; Olsen, D.; Carroll, S.; Embrey, E.; Wai, J.; Miller, M.; Cole, J. Inhibition of HIV-1 ribonuclease H by a novel diketo acid, 4-[5-(benzoylamino)thien-2-yl]-2,4-dioxobutanoic acid. *J. Biol. Chem.*, **2003**, *278*, 2777-2780.
- Tramontano, E.; Esposito, F.; Badas, R.; Di Santo, R.; Costi, R.; La Colla, P. 6-[1-(4-Fluorophenyl)methyl-1*H*-pyrrol-2-yl)]-2,4-dioxo-5-hexenoic acid ethyl ester a novel diketo acid derivative which selectively inhibits the HIV-1 viral replication in cell culture and the ribonuclease H activity *in vitro*. *Antiviral Res.*, **2005**, *65*, 117-124.
- Klumpp, K.; Mirzadegan, T. Recent progress in the design of small molecule inhibitors of HIV RNase H. *Curr. Pharm. Des.*, **2006**, *12*, 1909-1922.
- Borkow, G.; Fletcher, R. S.; Barnard, J.; Arion, D.; Motakis, D.; Dmitrienko, G. I.; Parniak, M. A. Inhibition of the ribonuclease H and DNA polymerase activities of HIV-1 reverse transcriptase by *N*-(4-*tert*-butylbenzoyl)-2-hydroxy-1-naphthaldehyde hydrazone. *Biochemistry*, **1997**, *36*, 3179-3185.
- Himmel, D.M.; Sarafianos, S.G.; Dharmasena, S.; Hossain, M.M.; McCoy-Simandle, K.; Iliina, T.; Clark, Jr. A.D.; Knight, J.L.; Julias, J.G.; Clark, P.K.; Krogh-Jespersen, K.; Levy, R.M.; Hughes, S.H.; Parniak, M.A.; Arnold, E. HIV-1 Reverse transcriptase structure with RNase H inhibitor dihydroxy benzoyl naphthyl hydrazone bound at a novel site. *ACS Chem. Biol.*, **2006**, *1*, 702-712.
- Singh, R.; Geetanjali; Chauhan, S.M.S. 9,10-Anthraquinones and Other Biologically Active Compounds from the Genus. *Rubia. Chem. Biodivers.*, **2004**, *1*, 1241-1264.
- Huang, Q.; Lu, G.; Shen, H.M.; Chung, M.C.; Onq, C.N. Anti-cancer properties of anthraquinones from Rhubarb. *Med. Res. Rev.*, **2007**, *27*, 609-630.
- Srinivas, G.; Babykutty, S.; Sathiadevan, P.P.; Srinivas P. Molecular mechanism of emodin effect: transition from laxative ingredient to antitumor agent. *Med. Res. Rev.*, **2007**, *27*, 591-608.
- Yim, H.; Lee, Y.H.; Lee, C.H.; Lee S.K. Emodine, an anthraquinone derivative isolated from the rhizomes of *Rheum palmatum*, selectively inhibits the activity of casein kinase II as a competitive inhibitor. *Planta Med.*, **1999**, *65*, 9-13.
- Koyama, M.; Takahashi, K.; Chou, T.C.; Darzynkiewicz, Z.; Kapuscinski, J.; Kelly, T.R.; Watanabe, K.A. Intercalating agents with covalent bond forming capability. A novel type of potential anti-cancer agents. 2. Derivatives of chrysophanol and emodine. *J. Med. Chem.*, **1989**, *32*, 1594-1599.
- Muller, S.O.; Lutz, W.K.; Sopper, H. Factors affecting the genotoxic potency ranking of natural anthraquinones in mammalian cell culture systems. *Mut. Res.*, **1998**, *414*, 125-129.
- Tan, J.H.; Zhang, Q.X.; Huang, Z.S.; Chen, Y.; Wang, X.D.; Gu, L.Q.; Wu, J.Y. Synthesis, DNA binding and cytotoxicity of new pyrazole emodin derivatives. *Eur. J. Med. Chem.*, **2006**, *41*, 1041-1047.
- Barnard, D.L.; Huffman, J.H.; Morris, J.L.B.; Wood, S.G.; Hughes, B.G.; Sidwell, R.W. Evaluation of antiviral activity of anthraquinones, anthrones and anthraquinone derivatives against human cytomegalovirus. *Antiviral Res.*, **1992**, *17*, 63-77.
- Shuangsoo, D.; Zhengguo, Z.; Yunru, C.; Xin, Z.; Baofeng, W.; Lichao, Y.; Yan'an, C. Inhibition of the replication of hepatitis B virus *in vitro* by emodine. *Med. Sci. Monit.*, **2006**, *12*, 302-306.
- Koyama, J.; Inoue, M.; Morita, I.; Kobayashi, N.; Osakai, T.; Nishino, H.; Tokuda, H. Correlation between reduction potentials and inhibitory effects on Epstein-Barr virus activation by emodine derivatives. *Cancer Lett.*, **2006**, *241*, 263-267.
- Farnet, C.M.; Wang, B.; Lipford, J.R.; Bushman, F.D. Differential inhibition of HIV-1 preintegration complexes and purified integrase protein by small molecules. *Proc. Natl. Acad. Sci. USA*, **1996**, *93*, 9742-9747.
- Deng, J.; Sanchez, T.; Neamati, N.; Briggs, J.M. Dynamic pharmacopore model optimization: identification of novel HIV-1 integrase inhibitors. *J. Med. Chem.*, **2006**, *49*, 1684-1692.
- Starnes, M.C.; Cheng, Y-C. Human immunodeficiency virus reverse transcriptase-associated RNase H activity. *J. Biol. Chem.*, **1989**, *264*, 7073-7077.
- Tramontano E.; Cheng, Y-C. HIV-1 reverse transcriptase inhibition by dipyrroldiazepinone derivative: BI-RG-587. *Biochem. Pharmacol.*, **1992**, *43*, 1371-1376.
- Yonetani, T. The Yonetani-Theorell graphical method for examining overlapping subsite of enzyme centers. *Methods Enzymol.*, **1982**, *87*, 500-509.
- Elion, G.B.; Singer, S.; Hitchings, G.H. Antagonists of nucleic acid derivatives. VIII. Synergism in combinations of biochemically related antimetabolites. *J. Biol. Chem.*, **1954**, *208*, 477-488.
- Dezinot, F.; Lang, R. Rapid colorimetric assay for cell growth and survival. *J. Immunol. Methods*, **1986**, *89*, 271-277.

- [28] Mellors, J.W.; Dutschman G.E.; Im G.-J.; Tramontano E.; Winkler S.R.; Cheng Y-C. *In vitro* selection and molecular characterization of human immunodeficiency virus-1 resistant to non-nucleoside inhibitors of reverse transcriptase. *Mol. Pharmacol.*, **1992**, *41*, 446-451.
- [29] Larder, B. A.; Chesebro, B.; Richman, D.D. Susceptibilities of zidovudine -susceptible and -resistant human immunodeficiency virus isolates to antiviral agents determined by using a quantitative plaque reduction assay. *Antimicrob. Agents Chemother.*, **1990**, *34*, 436-441.
- [30] Rice, P.; Craigie, R.; Davies, D.R. Retroviral integrases and their cousins. *Curr. Opin. Struct. Biol.*, **1996**, *6*, 76-83.
- [31] Rice, P.A.; Baker, T.A. Comparative architecture of transposase and integrase complexes. *Nat. Struct. Biol.*, **2001**, *8*, 302-307.
- [32] Hang, Q.L.; Li, Y.; Yang, Y.; Cammack, N.; Mirzadegan, T.; Klumpp, K. Substrate-dependent inhibition or stimulation of HIV RNase H activity by non-nucleoside reverse transcriptase inhibitors (NNRTIs). *Biochem. Biophys. Res. Comm.*, **2007**, *352*, 341-350.
- [33] Shaw-Reid, C.A.; Feuston, B.; Munshi, V.; Getty, K.; Jrueger, J.; Hazuda, D.J.; Parniak, M.A.; Miller, M.D.; Lewis, D. Dissecting the effects of DNA polymerase and ribonuclease H inhibitor combinations on HIV-1 reverse-transcriptase activities. *Biochemistry*, **2005**, *44*, 1595-1606.
- [34] Gopalakrishnan, V.; Benkovic, S. Human immunodeficiency virus type 1 reverse transcriptase: spatial and temporal relationship between the polymerase and RNase H activities. *Proc. Natl. Acad. Sci. USA*, **1992**, *89*, 10763-10767.
- [35] Palaniappan, C.; Fay, P.J.; Bambara, R.A. Nevirapine alters the cleavage specificity of ribonuclease H of human immunodeficiency virus 1 reverse transcriptase. *J. Biol. Chem.*, **1995**, *270*, 4861-4869.
- [36] Mohan, P.; Loya, S.; Avidan, O.; Verma, S.; Dhindsa, G.S.; Wong, M.F.; Huang, P.P.; Yashiro, M.; Baba, M.; Hizi, A. Synthesis of naphthalenesulfonic acid small molecules as selective inhibitors of the DNA polymerase and ribonuclease H activities of HIV-1 reverse transcriptase. *J. Med. Chem.*, **1994**, *37*, 2513-2519.
- [37] Min, B-S.; Miyashiro, H.; Hattori, M. Inhibitory effects of quinones on RNase H activity associated with HIV-1 reverse transcriptase. *Phytother. Res.*, **2002**, *16*, S57-S62.

---

Received: 29 April, 2009

Revised: 24 July, 2009

Accepted: 24 July, 2009